ChemPubSoc Europe

DOI: 10.1002/cplu.202000045

CHEMPLUSCHEM Full Papers

Phosphoprotein Detection with a Single Nanofluidic Diode Decorated with Zinc Chelates

Saima Nasir,[a, b] Mubarak Ali,*[a, b] Ishtiaq Ahmed,[c, d] Christof M. Niemeyer,[c] and Wolfgang Ensinger[a]

We report a nanofluidic device for the label-free detection of phosphoprotein (PPn) analytes. To achieve this goal, a metal ion chelator, namely 4-[bis(2-pyridylmethyl)aminomethyl]aniline (DPA–NH_2) compound was synthesized. Single asymmetric nanofluidic channels were fabricated in polyethylene terephthalate (PET) membranes. The chelator (DPA–NH_2) molecules are subsequently immobilized on the nanochannel surface, followed by the zinc ion complexation to afford DPA–Zn^{2+} chelates, which act as ligand moieties for the specific binding of phosphoproteins. The success of the chemical reaction and biomolecular recognition process that occur in a confined geometry can be monitored from the changes in electrical readout of the nanochannel. The nanofluidic sensor has the ability to sensitively and specifically detect lower concentrations ($\geq$1 nM) of phosphoprotein (albumin and α-casein) in the surrounding environment as evidenced from the significant decrease in ion current flowing through the nanochannels. However, dephosphoproteins such as lysozyme and dephospho-α-casein even at higher concentration ($>$1 μM) could not induce any significant change in the transmembrane ion flux. This observation indicated the sensitivity and specificity of the proposed nanofluidic sensor towards PPn proteins, and has potential for use in differentiating between phosphoproteins and dephosphoproteins.

Introduction

The solid-state nanochannels/nanopores exhibit higher stability (chemical or mechanical) compared to biological ion channels. The synthetic nanochannels have been successfully employed to mimic the functionality of ion channels.[1] Moreover, they also act as sensors. In this context, much attention has been devoted to miniaturize the nanofluidic based sensing devices during the recent years.[2] In the nanofluidic systems, the analyte sensing/recognition mainly depends on the nature of chemical groups (ligands) immobilized on the inner channel walls. These groups act as binding sites, and interact also with ionic species passing through the channel.[3] The biorecognition events are visualized from the changes in ion currents originating either from the passage of an analyte through the channel under an applied voltage or from the ligand-receptor interactions occurring inside the confined channel. Various methods have already been developed to introduce recognition units inside confined geometries for the detection of different (bio)molecules.[4] The biomolecular recognition process relies on the traditional ligand-receptor interactions such as protein–protein, biotin–streptavidin/avidin, antigen–antibody, and peptide nucleic acid–DNA complexes.[3a–g,4d–g] Moreover, synthetic nanochannels also have the ability to selectively detect a specific ionic moiety by the functionalization of desired ion responsive molecules on the channel surface.[5]

Among the various proteins/enzymes, phosphoprotein (PPn) plays a vital role in different biological processes including signal transduction, metabolic pathways, gene transcription, membrane transport, and others occurring in living organisms.[6] In both prokaryotic and eukaryotic organisms, phosphorylation/dephosphorylation of protein takes place in response to extracellular signals to regulate the enzymatic functions via conformational changes in their structures.[7] The process of phosphorylation/dephosphorylation of protein is frequently studied in bioanalytical and medicinal chemistry. It is foremost important to design molecular probes/ligands and develop versatile technique to recognise phosphoprotein of interest.

To date, the detection of phosphorylated (bio)molecules is mainly achieved by using antibodies and fluorescent techniques.[8] Although the antibody based method has been successfully employed in flow cytometry and immunohistochemistry in the cellular system of living organisms.[9] But, the use of antibody approach is limited because of the large size of the antibody which sometimes interfere in the structure and

[a] Dr. S. Nasir, Dr. M. Ali, Prof. W. Ensinger
Technische Universität Darmstadt
Fachbereich Material- u. Geowissenschaften
Fachgebiet Materialanalytik
Alarich-Weiss-Str. 2
64287 Darmstadt (Germany)
E-mail: m.ali@ma.tu-darmstadt.de
[b] Dr. S. Nasir, Dr. M. Ali
GSI Helmholtzzentrum für Schwerionenforschung
Planckstr. 1
64291 Darmstadt (Germany)
E-mail: M.Ali@gsi.de
[c] Dr. I. Ahmed, Prof. C. M. Niemeyer
Karlsruhe Institute of Technology (KIT)
Institute for Biological Interfaces (IBG-1)
Hermann-von-Helmholtz-Platz
76344 Eggenstein-Leopoldshafen, Germany
[d] Dr. I. Ahmed
University of Cambridge
Department of Chemical Engineering and Biotechnology
Philippa Fawcett Drive
Cambridge CB3 0AS (United Kingdom)

function of phosphoprotein. For the case of fluorescent/colorimetric technique, Zn(II)-coordinated dipicolylamine (DPA–Zn^{2+}) chelates have been proved effective receptors for phosphoprotein recognition.[10] But in this approach, the presence of a chromophore/fluorophore moiety (signalling unit) directly linked with the receptor (binding unit) is required to monitor the changes in light absorption or emission (or colour change/fluorescence change) on the binding of specific phosphorylated (bio)molecule.[8c] To overcome the above mentioned restrictions, the design and synthesis of alternative receptors which can be used for the antibody- and label-free phosphoprotein recognition are still at preliminary stages. Recently, we have demonstrated the detection of a small negatively charged pyrophosphate (PPi) molecule with synthetic nanochannels functionalized with bis(Zn^{2+}–DPA) complexes.[11] Later on, Jiang and his co-workers also demonstrated the detection of PPi anion by using the terpyridine–zinc (TPYD–Zn^{2+}) complexes immobilized on the single channel surface.[12]

Compared to the antibody and optical detection methods, our sensing technique relies on confining the sensing reaction into a volume of single channel which offers a simple method to recognize protein analyte through host guest interactions. Moreover, the electronic readout is very easy to follow by using simple experimental setup (picoammeter and voltage source).

In this study, we demonstrate a nanofluidic diode sensor for specific phosphoprotein (PPn) recognition in confined geometries. To this end, the interior of the nanochannel is tailored with dipicolylamine–zinc (DPA–Zn^{2+}) chelates. The metal complexes act as recognition elements for the capturing of PPn molecules (Figure 1). The sensing device has the ability to specifically recognize phosphoproteins (albumin and α-casien). On the contrary, it did not show significant response to other control proteins (lysozyme and dephospho-α-casien). The success of chemical reactions and biorecognition events occurring in confined environment are monitored from the changes in ion current flowing through the nanochannel.

Results and Discussion

Single asymmetric nanochannels are prepared in heavy ion irradiated 12 μm thick PET foils through asymmetric chemical etching of the damage trails caused by the energetic ions along their trajectories.[13] The irradiation and chemical track-etching process resulted in the generation of carboxyl (–COO^-) groups on the channel surface. Under physiological conditions, the ionized carboxylate (–COO^-) groups import negative charges to the channel surface. When negatively charged asymmetric channel is in contact with an electrolyte solution, the cavity of the cone is mainly filled with the cations (counter-ions). Under positive potential ($V > 0$) the electric field drag the cations toward narrow channel region and subsequently, the cations preferentially transported from tip to base side of the cone. While anions electrostatically prohibited to enter the nanochannel. For the case of negative potential ($V < 0$), the electric

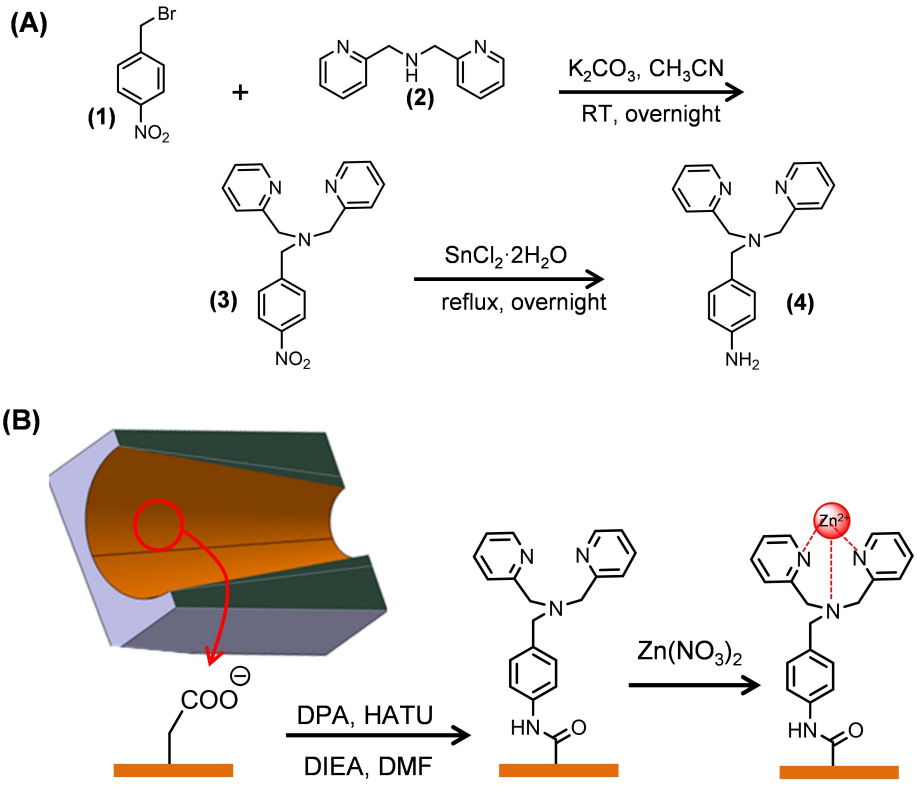

Figure 1. (A) Synthesis of the amine-terminated DPA chelator (DPA–NH_2). (B) Nanochannel surface functionalization with amine-terminated DPA molecules, and subsequent Zn^{2+} ion complexation.

field derive the cations away from the small opening of the cone.[14] Therefore, under applied bias higher value of ionic current is noticed at positive voltages compared to the negative one. This non-ohmic behavior is termed as ionic current rectification - a unique characteristic of asymmetric nanochannels.[5e,14–15] The polarity of the fixed chemical groups on the channel surface decides the direction of ion current rectification.

Moreover, the carboxylic acid groups on the channel surface serve as sites for the linkage of desired ligand molecules having primary amine in their backbone. For the capturing of (bio) molecule, first step is to design and synthesize a suitable ligand molecule. In this study, we have synthesized a dipicolylamine (DPA–NH_2) based metal ion chelator by following the reaction scheme shown in Figure 1A. To this end, the 4-nitrobenzyl bromide is reacted with di-(2-picolyl)amine to obtain the DPA nitrobenzene (DPA–NO_3) derivative.[16] Then the reduction of nitro group yields the DPA–NH_2 chelator.

After the synthesis of ligand, we proceeded to the immobilization of DPA–NH_2 molecules on the channel surface. The DPA–NH_2 molecule is first covalently attached on the channel surface by using a single step reaction process through HATU (hexafluorophosphate azabenzotriazole tetramethyl uronium) coupling chemistry. The HATU reagent in the presence of DIEA base converts the channel carboxylic acid groups into activated esters which immediately react with amine groups of the DPA–NH_2 chelator. Then the zinc (Zn^{2+}) ion complexation with the DPA moieties is carried out by exposing the DPA-modified membrane to $Zn(NO_3)_2$ solution.

Figure 2A shows the mechanism of phosphoprotein recognition and bioconjugation on the channel surface. The *I–V* characteristics of the single nanofluidic channel prior to and after the immobilization of DPA–Zn^{2+} chelates on the channel surface are shown in Figure 2B. For this purpose, the single-channel membrane is assembled between the two compartments of conductivity cell. The electrolyte (0.1 M KCl, pH 7.2) solution is filled on both sides of the membrane. For *I–V* measurements, the ground electrode is facing the base opening and working electrode on the tip opening side of the channel. With this electrode configuration higher value of ionic current is obtained at positive voltages when a potential applied across the membrane. Due to the presence of native carboxylate groups, as-prepared channel exhibits current rectification. For the case of modified channel, it is clearly evidenced from the current response that DPA–Zn^{2+} complexes impart positive charges to the channel surface, leading to the inversion of current rectification due to the switching of channel permselectivity from cation to anion.

The immobilized DPA–Zn^{2+} chelates served as recognition elements for the detection of phosphoproteins.[10d] The sensitivity and the selectivity (specificity) are the main analytical parameters which should be taken into account when designing a biosensing device. The sensing capability of the nanofluidic sensor is studied by exposing the modified channel to an electrolyte solution containing dephospho- and phosphor–protein analyte. To verify the specificity, the nanofluidic diode sensor is exposed to an electrolyte solution containing nonphosphorylated protein, *i.e.*, lysozyme and dephospho-α-casein, respectively. From the recordings of *I–V* curves as provided in Figure 2C clearly shows that the presence of these proteins in the background electrolyte could not induce any significant change in the ionic flux across the membrane. This confirmed the lack of binding capability of nonphosphorylated proteins toward the DPA–Zn^{2+} chelate. Thus the original surface remains undisturbed with the free coordination sites of metal cations in the DPA–Zn^{2+} chelate for binding with analyte of interest. Subsequently, when the same channel is exposed to albumin protein, bioconjugation occurred in the confined geometry due to the specific coordination of Zn^{2+} ion with the phosphoryl moieties in protein analyte. This biorecognition process leads to significant change in the ion current flowing through the modified nanofluidic channel (Figure 2D).

The sensitivity of the nanofluidic sensor is also tested against various albumin concentrations. As expected, even a very low albumin concentration resulted in a drastic decrease in the channel ion current, indicating the binding of albumin to the chelated zinc ion inside confined geometry as seen in Figure 2D. The observed decrease in the ionic current is attributed to the formation of bioconjugates onto the inner channel surface (Figure 2A). By increasing the albumin concentration, a further decrease in ionic current is noticed. It is evident from Figure 2D that the channel surface becomes saturated with bioconjugates at ~100 nM albumin concentration in the surrounding electrolyte. Further increase in protein concentration did not induce significant change in the ionic current flowing through the channel. Moreover, bioconjugation process occurring on the channel surface also modulate the rectification degree (f_{rec}) which is obtained from the ratio of higher currents to that of lower currents at given potential. Inset in Figure 2D shows the changes in rectification ratio (f_{rec}) values versus voltages calculated as $|I(-V)|/|I(+V)|$ for blank and 1 nM albumin concentration (because the current at negative potential is higher compared to that of positive one). Although, a significant decrease in ion current is noticed on exposure to 1 nM albumin concentration (Figure 2D) but we did not observe any significant change in the f_{rec} values when compare to blank solution. While, when the channel is exposed to electrolyte solution containing 10 nM albumin concentration, the direction of ion current rectification and f_{rec} values obtained as $|I(+V)|/|I(-V)|$) are switched from negative to positive which shows that the bioconjugation process import negative charges on the channel surface. Further increase in albumin concentrations to 100 nM and then 500 nM lead to almost blockage of channel and therefore, the f_{rec} values ($|I(+V)|/|I(-V)|$) are almost ~1 due to hindered flow of ions across the nanochannel. Note that from the *I–V* response and f_{rec} values shown in Figure 2D, it is very hard to find a linear relation in the change of current or f_{rec} versus different albumin protein concentrations due to current fluctuation/instabilities. The previously reported results also showed that bioconjugation in confined geometries clogged the tip opening, leading to the partial/permanent blockage of the ion current.[3a,4d,e,g,17] Figure 2E showed significant decrease in ion current measured at a

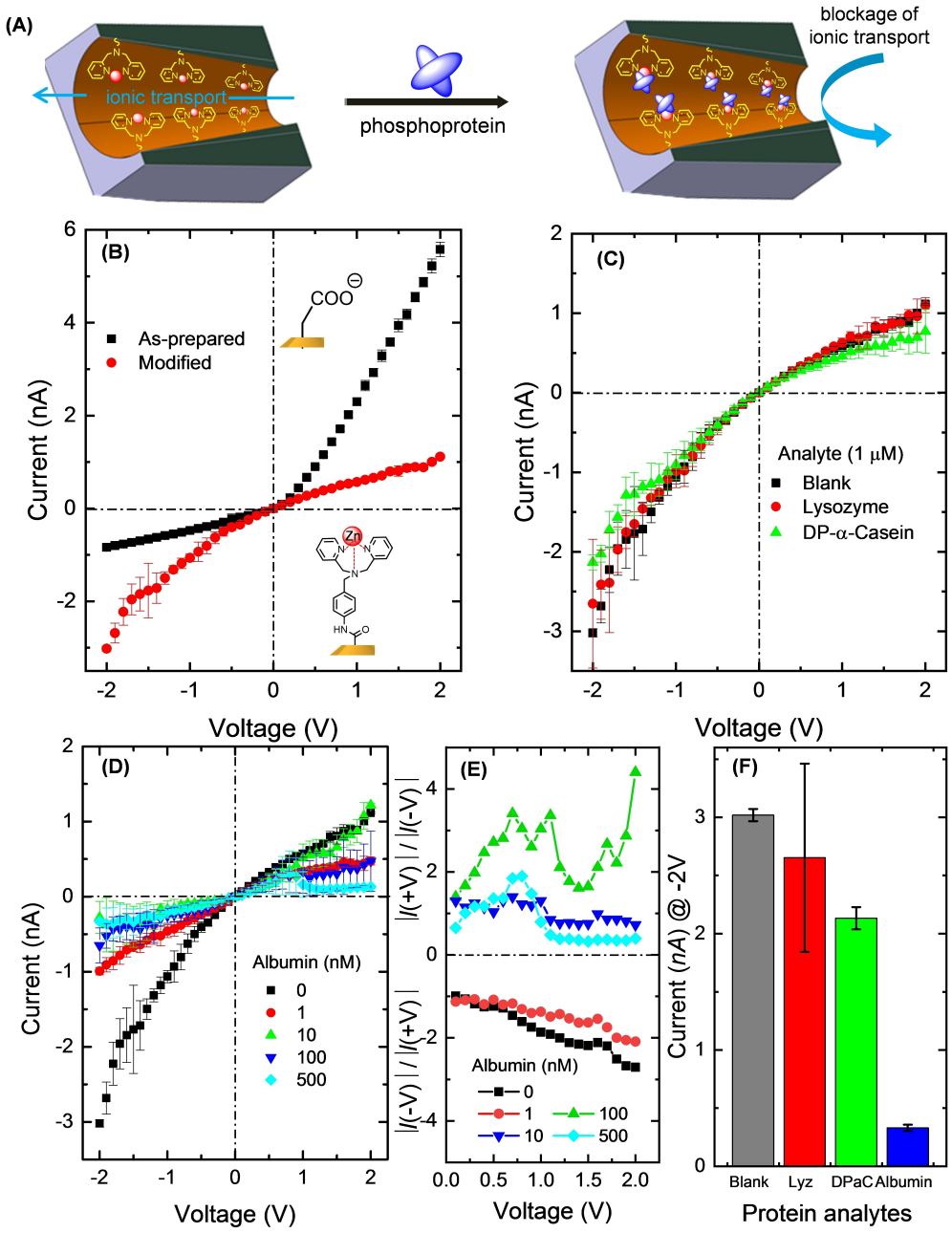

Figure 2. (A) Selective recognition and bioconjugation of phosphoprotein in confined geometries. (B) *I–V* characteristics of as-prepared and DPA–Zn^{2+}-modified single conical nanochannel ($d \sim 15$ nm and $D \sim 600$ nm). (C) *I–V* characteristics of the modified channel upon exposing to electrolyte solutions containing lysozyme and dephospho-α-casein proteins, separately. (D) *I–V* curves of DPA–Zn^{2+}-modified channel on exposure to electrolyte solution containing various concentrations of albumin protein. (E) Voltages versus current rectification ratio (f_{rec}) calculated as $|I(-V)|/|I(+V)|$ for blank and 1 nM albumin concentration, while for other albumin concentrations (10, 100 and 500 nM), the f_{rec} values are obtained as $|I(+V)|/|I(-V)|$. (F) The changes in ionic current measured at a potential of −2 V prior to (blank) and after exposure to various protein solutions, *i.e.*, lysozyme (1 μM), diphosphonate-α-casein (1 μM) and albumin (0.5 μM).

potential of −2 V on exposure to electrolyte solution containing phosphoprotein (albumin) and nonbinding (lysozyme and dephospho-α-casein) proteins. From the experimental data provided in Figure 2, we can infer that the presented nanofluidic diode sensor exhibits a remarkable sensitivity and specificity towards albumin because of possession of phosphate groups in the protein molecules.

To evaluate the reproducibility of the nanofluidic sensor, another nanochannel is modified with DPA–Zn^{2+} chelates and then exposed to phospho-α-casein under similar experimental parameters. Figure 3A shows the changes in current response of the nanofluidic sensor in the presence of various concentrations of phospho-α-casein protein in electrolyte solution.

Note that at lower protein concentrations, a decrease in ion current together with the current instabilities is observed,

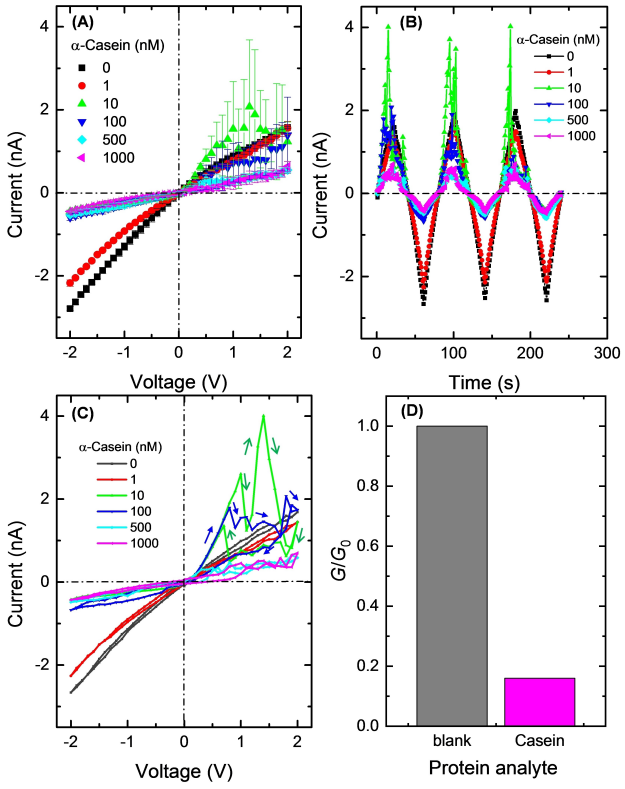

Figure 3. (A) *I–V* curves and (B) current vs time response and (C) ion current hysteric behaviour of modified channel ($d \sim 13$ nm and $D \sim 750$ nm) on exposure to an electrolyte solution having various concentrations of phospho-α-casein protein. (D) The channel conductance normalized to maximum conductance prior to (blank) and after exposure to α-casein protein solution (1 μM).

indicating the interaction of proteins with the binding sites on channel walls. Figure 3B clearly shows the reversible change in current vs time curves under applied voltages in the range (+ 2 V, −2 V). The hysteric behavior of ion current in one complete cycle of *I–V* curve is provided in Figure 3C. At lower protein concentrations (10 and 100 nM), the hysteric effect appeared at higher voltages. The arrows show the direction of the *I–V* recordings with increasing time. It was reported that transient changes in the channel fixed charges are responsible for ion current fluctuations.[18] Higher protein concentrations (≥ 100 nM) lead to the origination of more bioconjugates, which ultimately cause steric obstruction of the channel tip opening and consequently, a reduction/blockage of the ionic current was noticed.

The experimental results (Figures 2 and 3) proved that the proteins having different molecular weights/chemical composition can be identified based on the changes in electrical readout of the nanochannel. Although in both cases, nanofluidic sensor exhibits current instabilities and fluctuations might be due to the adsorption/desorption of protein analyte on the channel surface or passage of protein molecule through the nanochannel interrupt the ion flow under applied potential. But for the case of albumin, the current instabilities noticed even at lower concentration as can be seen from the error bar provided in Figure 2D. While in the case of casein, current blockage/instabilities observed at higher concentration (Figure 3). This difference in electrical signal is mainly due to different molecular sizes of both proteins. Note that the molecular weight of the albumin (~44.3 kDa)[19] is almost double compared to phospho-α-casein (~22 kDa).[20]

We have also performed the experiment under asymmetric addition of protein analyte in the electrolyte solution. For this purpose, DPA–Zn^{2+}-modified channel is fixed in a conductivity cell. An electrolyte solution containing phospho-α-casein (100 mM KCl + protein) is filled on the tip side while the base side of modified channel remain exposed to blank electrolyte (100 mM KCl) solution. Figure 4A shows the *I–V* characteristics of the modified nanochannel whose tip region is exposed to various concentration of phospho-α-casein. It can be seen that at lower protein concentration (1 to 10 nM), we did not notice any significant change in the *I–V* curve, indicating the presence of insufficient protein molecules required to induce significant change in the ion flow. By increasing the phospho-α-casein concentration to 100 nM, bioconjugation occurred on the tip side which lead to current rectification much similar to negatively charged asymmetric channel. Note that the isoelectric point (*pI* ~4.44) of α-casein is lower than the pH (7.2) conditions used in the present study. Therefore, the binding of α-casein import negative charge to the tip region, resulting the rectification of ion current flowing through the nanochannel. Upon increasing the α-casein concentration from 100 to 500 nM, a further increase in rectified ion flux is noticed. At higher α-casein concentration (1 μM), a decrease in rectified ion flux along with fluctuation is observed due to accumulation of protein at the tip regions, obstructing the flow of ions across the membrane. On exposure to more concentrated solution (results not shown here), the bioconjugation process clogged the tip opening, leading to almost blockage of the ion current. Previously, Siwy and her co-workers have also reported that the asymmetric binding of protein molecules induce change in the channel polarity which in turn switched the current rectification phenomenon of the nanochannel.[21] Moreover, Karnik *et al.* have also demonstrated that the analyte molecular charge

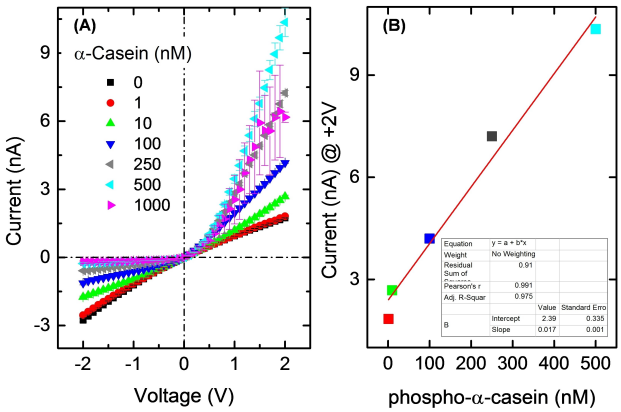

Figure 4. (A) *I–V* characteristics of asymmetric nanochannel ($d \sim 30$ nm and $D \sim 486$ nm) modified DPA–Zn^{2+} on exposure to electrolyte solutions containing various concentrations of phospho-α-casein only on the tip side of single asymmetric nanochannel. (B) Changes in the ion current versus phospho-α-casein concentrations (1–500 nM) at a potential of + 2 V.

dominate at lower concentrations while at higher concentrations volume exclusion effect dominate due to the formation of bioconjugates in confined geometries.[22] Figure 4B shows the changes in the ion current versus protein concentrations obtained at the positive potential (+2 V). The rectified ion current increased almost in a linear fashion up to 500 nM concentration of α-casein. Thus the preseneted nanofluidic sensor also provides quantitative information on the protein concentrations down to nanomolar range.

It is worth to mention that the data presented in Figure 2 and Figure 3 exhibits instabilities and fluctuation in the electrical signal of the nanofluidic sensor because of very small opening (≤15 nm) of the asymmetric nanochannel. Moreover, the modified channel exposed to symmetric electrolyte condition, *i.e.,* protein is added on both sides of the channel. While for the case of Figure 4, the tip opening diameter (~30 nm) is almost double and the protein is added only on one side, i.e., cone tip side of the conical nanochannel. Therefore, the ionic transport through the channel is now dictated mainly by the charge of bioconjugates formed on the channel surface.

On the contrary, a nanofluidic channel functionalized with zinc complexes comprised of two di(2-picolyl)amine [bis(Zn^{2+}–DPA)] has the ability to sense picomolar concentration of pyrophosphate anion (PPi) in the surrounding electrolyte as evidenced from the change in permselectivity of the nanochannel.[11] While, the nanofluidic sensor could not show significant response on exposure to other phosphate anions such as monohydrogen phosphate, dihydrogen phosphate, adenosine monophosphate (AMP), adenosine diphosphate (ADP) and adenosine triphosphate (ATP) even at higher concentrations.

Finally, we have also performed a negative control experiment under the same set of experimental conditions by using an as-prepared (carboxylated) and DPA-modified nanochannel. The as-prepared (unmodified) conical channel exhibits ion current rectification due to the presence of fixed negative charges (COO–) on the channel surface (Figure 5A). After chemical modification, the channel surface charge is reduced due to the presence of uncharged DPA moieties on the channel walls. This lead to significant decrease in rectified ion flux as evidenced from the *I–V* curve (Figure 5B). It is evident from the *I–V* response shown in Figure 5 that even higher protein concentrations could not induce any significant change in rectified ion flux across the membrane. These experimental results further supported our finding that the phosphoproteins can only specifically bind with recognition moieties (DPA–Zn^{2+}) on the channel surface.

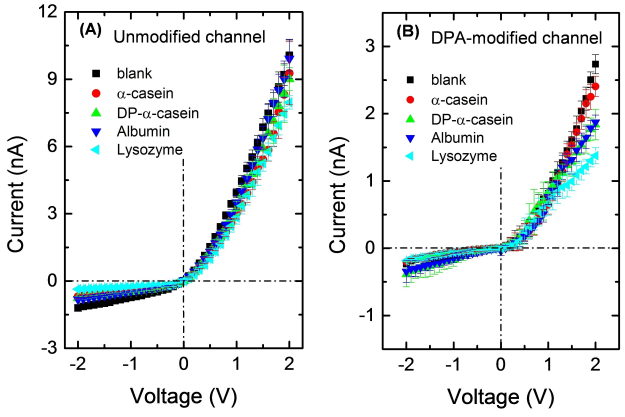

Figure 5. *I–V* curves of the single asymmetric channel before (A) and after DPA-modification (B) measured in presence of a 10 μM concentration of various proteins in electrolyte solution.

The nanofluidic sensor demonstrated here are not reusable because of irreversible binding in between DPA–Zn^{2+} and phosphoprotein. For reuse of such sensor, exposure to strongly acidic solution (pH≤3) is required to dissociate bioconjugates from the nanofluidic channel. But under these conditions, the metal complex (DPA–Zn^{2+}) can also be dissociated due to protonation of nitrogen groups on the DPA molecule, leaving DPA moieties on the channel surface. There would be a possibility to recomplex the metal ion to regenerate the DPA–Zn^{2+} chelates on the channel surface for the detection of phosphoprotein analytes. But there would be some limitation in the reuse of such nanofluidic sensor: a) it is not sure that all the bioconjuagtes will be dissociated and washed out from the channel surface. b) on exposure to strong acidic solution and re-complexation of metal ion, the tip opening (sensing zone) of the conical nanochannels could be damaged or deformed.

Conclusion

In summary, we have demonstrated the phosphoprotein recognition/conjugation in confined geometries. To this end, DPA–NH_2 was synthesized and immobilized on the channel surface followed by the complexation of zinc ion to generate DPA–Zn^{2+} complexes which acted as an artificial ligand for the binding of phosphoproteins. The nanofluidic channel modification and biomolecular recognition processes occurring in confined environment were monitored through *I–V* measurements. Significant changes in the ion flux occurred when the nanofluidic sensor was exposed to an electrolyte solution containing phosphoprotein even in the nanomolar (nM) concentration range. In contrast, control proteins such as lysozyme and dephospho-α-casein could not induce any significant change in the transmembrane ion flux. This indicated the sensitivity and specificity of the proposed nanofluidic sensor towards almost all biomolecules having phosphate moieties in their backbone. In this context, we believe that metal affinity-based nanofluidic biosensors would readily be used to differentiate between phospho- and dephospho-proteins based on the changes in the electronic read-out originated by the ionic transport through the channel.

Materials and methods

Materials

All the chemicals, including di-(2-picolyl)amine (DPA, 97%), 4-nitrobenzylbromide (99%), lysozyme from chicken egg white

(product number L6876), albumin from chicken egg white (product number A5503), α-casein from bovine milk (product number C6780), α-casein dephosphorylated from bovine milk (DP-α-casein, product number C8032) *N*,*N*-dimethylformamide (DMF, 99.8%), *N*,*N*-diisopropylethylamine (DIEA, 99.5%), 1-[bis(dimethylamino) methylene]-1*H*-1,2,3-triazolo[4,5-*b*]pyridinium-3-oxid hexafluorophosphate (HATU, 97%), *N*-(2-hydroxyethyl)piperazine-*N*′-(2-ethanesulfonic acid) (I M HEPES, pH 7.0–7.6) solution and zinc nitrate hexahydrate ($Zn(NO_3)_2 \cdot 6H_2O$) as well as all the solvents were purchased from Sigma-Aldrich, Taufkirchen, Germany, and were used without further purification.

^1H and ^{13}C NMR spectra were recorded at 500 and 125 MHz in $CDCl_3$, respectively. High-resolution mass spectra were measured using Finnigan MAT90 mass spectrometer. Analytical TLC (silica gel, 60F-54, Merck) and spots were visualized under UV light and/or phosphomolybdic acid–ethanol. Flash column chromatography was performed with silica gel 60 (70–230 mesh, Merck) and basic aluminum oxide (activated, basic, ~150 mesh, 58 Å, Aldrich).

Polyethyleneterephthalate (PET) membranes (Hostaphan RN 12, Hoechst) of 12 μm thickness were irradiated at the GSI Helmholtz Centre for Heavy Ion Research (Darmstadt) with Au ions (energy: 11 MeV/u, ion fluence: either single or 10^7 ions cm^{-2}). Subsequently, the ion tracked PET membranes were further exposed to UV light from each side for 1 hour to sensitize the latent tracks for the etching process.

Fabrication of single asymmetric nanochannels

The heavy ion tracked PET membranes were chemical etched using an asymmetric track-etching technique developed by Apel and his co-workers.[13] A detailed procedure for the conversion of ion tracks into asymmetric channels was described previously. Briefly, ion tracked PET membrane was chemically etched from one side with an etching solution (9 M NaOH) at room temperature. While, the other side of the membranes was exposed to stopping solution to neutralize the etchant after the breakthrough. During the etching process, a voltage of 1 V was applied across the single ion tracked membrane to monitor the current flowing through the nascent channel. The etching process was terminated when the current had reached a certain value. After etching, etched membranes were immersed in deionized water to remove the residual salts.

Synthesis di-(2-picolyl)amine based chelator DPA–NH_2 (4)

The numbers of the different compounds in the synthesis of DPA chelator are identified in Figure 1A.[16]

Synthesis of compound (3)

Potassium carbonate (3.0 g, 21.73 mmol) was added to a solution of 4-nitrobenzylbromide (1.65 g, 7.63 mmol) dissolved in anhydrous CH_3CN (45 mL) and stirred for 20 minutes. Di-(2-picolyl)amine (1.0 g, 7.53 mmol) solution in CH_3CN (10 mL) was then added drop wise. The reaction mixture was stirred overnight under argon. The volatiles were removed under reduced pressure to obtain dark brown crude product. The residue was purified by silica gel flash column chromatography (CH_2Cl_2/MeOH, 50:1, v/v) to afford pure 4-[bis(2-pyridylmethyl)aminomethyl]nitrobenzene (3) as an orange oil (2.2 g, 6.58 mmol, 87% yield).

^1H NMR (500 MHz, $CDCl_3$): δ (ppm) 3.81 (s, 2H), 3.83 (s, 4H), 7.17 (m, 2H), 7.52 (d, J=7.8 Hz, 2H), 7.58 (d, J=8.7 Hz, 2H), 7.68 (td, J=7.8 Hz, 1.7 Hz, 2H), 8.15 (d, J=8.7 Hz 2H), 8.54 (m, 2H).

^{13}C NMR (125 MHz, $CDCl_3$): δ (ppm) 57.7, 60.1, 122.2, 123.0, 123.5, 129.4, 136.8, 147.0, 149.1, 158.8.

HRMS-FAB: calcd. for $C_{19}H_{19}N_4O_2$ $[M+H]^+$ 335.2451, found 335.2489

Synthesis of compound (4)

To a solution of 4-[bis(2-pyridylmethyl)aminomethyl]nitrobenzene (**3**) (1.53 g, 4.58 mmol) in ethanol (60 mL) was added tin chloride dihydrate (5.25 g, 22.55 mmol). The reaction mixture was refluxed for 16 hrs. The solvent was evaporated under reduced pressure to give the crude product. The residue was purified by silica gel column chromatography using 10% MeOH in dichloromethane to afford pure 4-[bis(2-pyridylmethyl)aminomethyl]aniline (**4**) as an orange oil (0.93 g, 3.98 mmol, 86% yield).

^1H NMR (500 MHz, $CDCl_3$): δ (ppm) 3.55 (s, 2H), 3.59 (bs, 2H), 3.73 (s, 4H), 6.61 (d, J=7.9 Hz, 2H), 7.12 (m, 2H), 7.15 (d, J=7.9 Hz, 2H), 7.55 (d, J=7.8 Hz,2H), 7.62 (m, 2H), 8.44 (d, J=8.6 Hz, 2H).

^{13}C NMR (125 MHz, $CDCl_3$): δ (ppm) 57.4, 60.1, 115.2, 122.0, 122.9, 128.7, 130.1, 136.4, 148.9, 160.2.

HRMS-FAB: calcd. for $C_{19}H_{21}N_4$ $[M+H]^+$ 305.2591, found 305.2537.

Chemical functionalization of channel surface with DPA–Zn^{2+} complexes

Carboxylic acid groups were generated on the channel surface because of the heavy ion irradiation and chemical etching. These functional moieties can be exploited for the covalent linkage of DPA–NH_2 molecule through HATU (Hexafluorophosphate Azabenzotriazole Tetramethyl Uronium) coupling chemistry. It is a single step reaction employed to functionalize the channel surface. To accomplish this goal, the DPA–NH_2 (10 mM), HATU (10 mM) and DIEA (5 mM) were dissolved in anhydrous DMF solvent. Then the polymer foil with single asymmetric channel was dipped in this solution under argon atmosphere for overnight at room temperature. The modified membrane was washed thoroughly first with DMF followed by careful rinsing with deionized water. The zinc ion complexation on channel surface was archived by exposing the DPA-modified membrane to an aqueous solution of $Zn(NO_3)_2$ (1 mM) for 2 hrs at room temperature.

Current-voltage measurements

As-prepared and modified single-channel membrane were fixed between the two halves of the conductivity cell, separately. Then an electrolyte solution (100 mM KCl) was filled on both sides of the membrane. The ionic current flowing through the single channel membrane was measured with a picoammeter/voltage source (Keithley 6487, Keithley Instruments, Cleveland, OH) through Ag/AgCl electrode placed into each half-cell solution. A scanning triangle voltage from −2 to +2 V was applied across the single-channel membrane to record the *I*–*V* curves.

Moreover, various concentrations of phosphoproteins (ablumin and α-casien) and control proteins (lysozyme and DP-α-casien) were prepared in the electrolyte (0.1 M KCl) solution (pH 7.2) and the corresponding *I*–*V* curves were recorded under symmetric and also asymmetric electrolyte conditions.

Acknowledgements

M.A., S.N. and W.E. acknowledge the funding from the Hessen State Ministry of Higher Education, Research and the Arts, Germany, under the LOEWE project iNAPO. I.A. and C.M.N. acknowledge financial support through the Helmholtz programme BioInterfaces in Technology and Medicine. The authors are thankful to Prof. C. Trautmann from GSI (Department of Material Research) for support with the heavy ion irradiation experiments.

Conflict of Interest

The authors declare no conflict of interest.

Keywords: biomolecules · ion current rectification · ligand-receptor interactions · sensors · synthetic nanochannels

[1] a) B. Hille, *Ionic channels of excitable membranes, 3rd ed.*, Sinauer Associates Inc., Sunderland, MA, **2001**; b) K. Xiao, K. Wu, L. Chen, X.-Y. Kong, Y. Zhang, L. Wen, L. Jiang, *Angew. Chem. Int. Ed.* **2018**, *57*, 151–155; *Angew. Chem.* **2018**, *130*, 157–161.

[2] a) K. Healy, *Nanomedicine* **2007**, *2*, 459–481; b) X. Hou, W. Guo, L. Jiang, *Chem. Soc. Rev.* **2011**, *40*, 2385–2401; c) X. Hou, H. C. Zhang, L. Jiang, *Angew. Chem. Int. Ed.* **2012**, *51*, 5296–5307; *Angew. Chem.* **2012**, *124*, 5390–5401; d) M. Lepoitevin, T. Ma, M. Bechelany, J.-M. Janot, S. Balme, *Adv. Colloid Interface Sci.* **2017**, *250*, 195–213; e) O. Graniel, M. Weber, S. Balme, P. Miele, M. Bechelany, *Biosens. Bioelectron.* **2018**, *122*, 147–159.

[3] a) M. Ali, S. Nasir, Q. H. Nguyen, J. K. Sahoo, M. N. Tahir, W. Tremel, W. Ensinger, *J. Am. Chem. Soc.* **2011**, *133*, 17307–17314; b) M. Ali, R. Neumann, W. Ensinger, *ACS Nano* **2010**, *4*, 7267–7274; c) M. Ali, Q. H. Nguyen, R. Neumann, W. Ensinger, *Chem. Commun.* **2010**, *46*, 6690–6692; d) C. C. Harrell, P. Kohli, Z. Siwy, C. R. Martin, *J. Am. Chem. Soc.* **2004**, *126*, 15646–15647; e) V. Horváth, T. Takécs, G. Horvai, P. Huszthy, J. S. Bradshaw, R. M. Izatt, *Anal. Lett.* **1997**, *30*, 1591–1609; f) K. B. Jirage, J. C. Hulteen, C. R. Martin, *Science* **1997**, *278*, 655–658; g) S. Umehara, M. Karhanek, R. W. Davis, N. Pourmand, *Proc. Natl. Acad. Sci. USA* **2009**, *106*, 4611–4616; h) Z. Y. Sun, T. B. Liao, Y. L. Zhang, J. Shu, H. Zhang, G. J. Zhang, *Biosens. Bioelectron.* **2016**, *86*, 194–201; i) Q. Q. Wang, H. M. Wang, X. Fan, J. Zhai, *Sci. Adv. Mater.* **2015**, *7*, 2147–2167; j) P. Li, X.-Y. Kong, G. Xie, K. Xiao, Z. Zhang, L. Wen, L. Jiang, *Small* **2016**, *12*, 1854–1858.

[4] a) L. A. Baker, S. P. Bird, *Nat. Nanotechnol.* **2008**, *3*, 73–74; b) L. A. Baker, Y. S. Choi, C. R. Martin, *Curr. Nanosci.* **2006**, *2*, 243–255; c) R. E. Gyurcsanyi, *TrAC Trends Anal. Chem.* **2008**, *27*, 627–639; d) M. Ali, P. Ramirez, M. N. Tahir, S. Mafe, Z. Siwy, R. Neumann, W. Tremel, W. Ensinger, *Nanoscale* **2011**, *3*, 1894–1903; e) M. Ali, B. Yameen, R. Neumann, W. Ensinger, W. Knoll, O. Azzaroni, *J. Am. Chem. Soc.* **2008**, *130*, 16351–16357; f) M. Lepoitevin, G. Nguyen, M. Bechelany, E. Balanzat, J.-M. Janot, S. Balme, *Chem. Commun.* **2015**, *51*, 5994–5997; g) Z. Siwy, L. Trofin, P. Kohli, L. A. Baker, C. Trautmann, C. R. Martin, *J. Am. Chem. Soc.* **2005**, *127*, 5000–5001; h) D. F. Ding, P. C. Gao, Q. Ma, D. G. Wang, F. Xia, *Small* **2019**, *15*; i) Q. Ma, Z. X. Si, Y. Li, D. G. Wang, X. L. Wu, P. C. Gao, F. Xia, *TrAC Trends Anal. Chem.* **2019**, *115*, 174–186; j) G. Perez-Mitta, A. S. Peinetti, M. L. Cortez, M. E. Toimil-Molares, C. Trautmann, O. Azzaroni, *Nano Lett.* **2018**, *18*, 3303–3310; k) A. de la Escosura-Muniz, A. Merkoci, *TrAC Trends Anal. Chem.* **2016**, *79*, 134–150.

[5] a) Y. Shang, Y. Zhang, P. Li, J. Lai, X.-Y. Kong, W. Liu, K. Xiao, G. Xie, Y. Tian, L. Wen, L. Jiang, *Chem. Commun.* **2015**, *51*, 5979–5981; b) Q. Liu, K. Xiao, L. Wen, H. Lu, Y. Liu, X.-Y. Kong, G. Xie, Z. Zhang, Z. Bo, L. Jiang, *J. Am. Chem. Soc.* **2015**, *137*, 11976–11983; c) Y. Tian, Z. Zhang, L. Wen, J. Ma, Y. Zhang, W. Liu, J. Zhai, L. Jiang, *Chem. Commun.* **2013**, *49*, 10679–10681; d) Y. Tian, X. Hou, L. Wen, W. Guo, Y. Song, H. Sun, Y. Wang, L. Jiang, D. Zhu, *Chem. Commun.* **2010**, *46*, 1682–1684; e) M. Ali, I. Ahmed, P. Ramirez, S. Nasir, J. Cervera, S. Mafe, C. M. Niemeyer, W. Ensinger, *Langmuir* **2017**, *33*, 9170–9177; f) M. Ali, I. Ahmed, P. Ramirez, S. Nasir, S. Mafe, C. M. Niemeyer, W. Ensinger, *Anal. Chem.* **2018**, *90*, 6820–6826; g) G. Perez-Mitta, A. G. Albesa, W. Knoll, C. Trautmann, M. E. Toimil-Molares, O. Azzaroni, *Nanoscale* **2015**, *7*, 15594–15598; h) P. Ramirez, J. Cervera, V. Gomez, M. Ali, S. Nasir, W. Ensinger, S. Mafe, *J. Membr. Sci.* **2019**, *573*, 579–587; i) P. Ramirez, J. A. Manzanares, J. Cervera, V. Gomez, M. Ali, I. Pause, W. Ensinger, S. Mafe, *J. Membr. Sci.* **2018**, *563*, 633–642; j) L. Yang, Y. Qian, X.-Y. Kong, M. Si, Y. Zhao, B. Niu, X. Zhao, Y. Wei, L. Jiang, L. Wen, *ACS Appl. Mater. Interfaces* **2020**, *12*, 3854–3861; k) W. Khalid, M. A. Abbasi, M. Ali, Z. Ali, M. Atif, C. Trautmann, W. Ensinger, *Electrochim. Acta* **2020**, *337*, 135810.

[6] L. N. Johnson, R. J. Lewis, *Chem. Rev.* **2001**, *101*, 2209–2242.

[7] a) M. Ashcroft, M. H. G. Kubbutat, K. H. Vousden, *Mol. Cell. Biol.* **1999**, *19*, 1751–1758; b) C. A. Khan, P. F. Fitzpatrick, *Biochemistry* **2018**, *57*, 6274–6277; c) H. Meng, M. C. Fitzgerald, *J. Proteome Res.* **2018**, *17*, 1129–1137.

[8] a) A. Ojida, T. Kohira, I. Hamachi, *Chem. Lett.* **2004**, *33*, 1024–1025; b) F. J. Williams, D. Fiedler, *ACS Chem. Biol.* **2015**, *10*, 1958–1963; c) A. E. Hargrove, S. Nieto, T. Zhang, J. L. Sessler, E. V. Anslyn, *Chem. Rev.* **2011**, *111*, 6603–6782.

[9] H. Zhang, X. M. Zha, Y. Tan, P. V. Hornbeck, A. J. Mastrangelo, D. R. Alessi, R. D. Polakiewicz, M. J. Comb, *J. Biol. Chem.* **2002**, *277*, 39379–39387.

[10] a) K. L. Haas, K. J. Franz, *Chem. Rev.* **2009**, *109*, 4921–4960; b) A. Hauser, M. Penkert, C. P. R. Hackenberger, *Acc. Chem. Res.* **2017**, *50*, 1883–1893; c) S. Lee, K. K. Y. Yuen, K. A. Jolliffe, J. Yoon, *Chem. Soc. Rev.* **2015**, *44*, 1749–1762; d) T. Minamiki, T. Minami, P. Koutnik, P. Anzenbacher, S. Tokito, *Anal. Chem.* **2016**, *88*, 1092–1095.

[11] M. Ali, I. Ahmed, P. Ramirez, S. Nasir, C. M. Niemeyer, S. Mafe, W. Ensinger, *Small* **2016**, *12*, 2014–2021.

[12] Y. Zhang, R. Zhou, Z. Zhao, X.-Y. Kong, G. Xie, Q. Liu, P. Li, Z. Zhang, K. Xiao, Z. Liu, L. Wen, L. Jiang, *ChemPhysChem* **2017**, *18*, 253–259.

[13] P. Y. Apel, Y. E. Korchev, Z. Siwy, R. Spohr, M. Yoshida, *Nucl. Instrum. Methods Phys. Res. Sect. B* **2001**, *184*, 337–346.

[14] a) J. Cervera, B. Schiedt, R. Neumann, S. Mafe, P. Ramirez, *J. Chem. Phys.* **2006**, *124*, 104706; b) Z. S. Siwy, *Adv. Funct. Mater.* **2006**, *16*, 735–746.

[15] a) M. Ali, P. Ramirez, S. Mafe, R. Neumann, W. Ensinger, *ACS Nano* **2009**, *3*, 603–608; b) X. Hou, L. Jiang, *ACS Nano* **2009**, *3*, 3339–3342; c) P. Ramirez, P. Y. Apel, J. Cervera, S. Mafe, *Nanotechnology* **2008**, *19*, 315707.

[16] P. Du, S. J. Lippard, *Inorg. Chem.* **2010**, *49*, 10753–10755.

[17] M. Ali, B. Schiedt, R. Neumann, W. Ensinger, *Macromol. Biosci.* **2010**, *10*, 28–32.

[18] a) Y. E. Korchev, C. L. Bashford, G. M. Alder, P. Y. Apel, D. T. Edmonds, A. A. Lev, K. Nandi, A. V. Zima, C. A. Pasternak, *FASEB J.* **1997**, *11*, 600–608; b) A. Wolf, Z. Siwy, Y. E. Korchev, N. Reber, R. Spohr, *Cell. Mol. Biol. Lett.* **1999**, *4*, 553–565.

[19] T. Tai, K. Yamashita, S. Ito, A. Kobata, *J. Biol. Chem.* **1977**, *252*, 6687–6694.

[20] W. N. Eigel, J. E. Butler, C. A. Ernstrom, H. M. Farrell, V. R. Harwalkar, R. Jenness, R. M. Whitney, *J. Dairy Sci.* **1984**, *67*, 1599–1631.

[21] I. Vlassiouk, T. R. Kozel, Z. S. Siwy, *J. Am. Chem. Soc.* **2009**, *131*, 8211–8220.

[22] R. Karnik, K. Castelino, R. Fan, P. Yang, A. Majumdar, *Nano Lett.* **2005**, *5*, 1638–1642.

Manuscript received: January 24, 2019
Accepted manuscript online: February 17, 2020